

---

---

# *Contents*

<b>Preface</b>	<b>ix</b>
<b>1 Introduction</b>	<b>1</b>
1.1 Concept of magnetic reconnection and its development	1
1.2 Recent development and progress of understanding magnetic reconnection	7
1.3 Major questions	10
<b>2 Magnetic reconnection observed in space and laboratory plasmas</b>	<b>14</b>
2.1 Magnetic reconnection in solar flares	14
2.2 Magnetic reconnection in the magnetosphere	21
2.3 Magnetic reconnection in self-organization in fusion plasmas	23
2.4 An observation of a prototypical reconnection layer in a laboratory experiment	28
<b>3 Development of MHD theories for magnetic reconnection, and key observations in laboratory and space plasmas</b>	<b>30</b>
3.1 Early history of MHD theory on magnetic reconnection	30
3.2 Description of plasma fluid in magnetic fields by MHD	32
3.3 The flux freezing principle and maintaining plasma equilibrium	33
3.4 Breakdown of flux freezing and magnetic reconnection	37
3.5 Resistive MHD theories and magnetic reconnection	38
3.6 Experimental analysis of the magnetic reconnection layer based on MHD models	46
<b>4 Kinetic description of the reconnection layer: One-dimensional Harris equilibrium and an experimental study</b>	<b>55</b>
4.1 One-dimensional Harris formulation and solutions	55
4.2 Theory of the generalized Harris sheet	56
4.3 Experimental investigation of the Harris sheet	59
4.4 Additional comments and discussion	63
<b>5 Development of two-fluid theory for reconnection coordinated with key observations</b>	<b>65</b>
5.1 Reconnection in the magnetosphere and two-fluid dynamics	65
5.2 Relationship between the two-fluid formulation and MHD	66

5.3	Development of particle-in-cell simulations	68
5.4	Results from two-dimensional numerical simulations for collisionless reconnection	69
5.5	Profile and characteristics of the two-fluid reconnection layer	77
5.6	Experimental observations of two-fluid effects in the reconnection layer	79
5.7	Observation of a two-scale reconnection layer with identification of the electron diffusion layer in a laboratory plasma	86
5.8	Waves in the reconnection layer and enhanced resistivity	89
<b>6</b>	<b>Laboratory plasma experiments dedicated to the study of magnetic reconnection</b>	<b>98</b>
6.1	Early laboratory experiments on reconnection	98
6.2	Experiments of toroidal plasma merging	102
6.3	Controlled driven reconnection experiments	109
6.4	Main facilities dedicated to reconnection study	116
<b>7</b>	<b>Recent observations of magnetic reconnection in solar and astrophysical plasmas</b>	<b>117</b>
7.1	Features of magnetic reconnection in solar flare eruptions	117
7.2	Development of the standard solar flare model and magnetic reconnection	119
7.3	Breakout model with a multipolar magnetic configuration	123
7.4	Magnetic reconnection occurs impulsively	127
7.5	A model of magnetic reconnection in the Crab Nebula	130
7.6	Notes on fast collisionless reconnection in space astrophysical plasmas	133
<b>8</b>	<b>Recent observations of magnetic reconnection in space astrophysical plasmas</b>	<b>135</b>
8.1	Magnetic reconnection layer in the magnetosphere	135
8.2	Observational studies of magnetic reconnection in the magnetosphere with the aid of numerical simulations	137
8.3	Electron-scale measurements of the reconnection layer in the magnetopause	140
8.4	Electron-scale dynamics of the symmetric reconnection layer in the magnetotail	146
<b>9</b>	<b>Magnetic self-organization phenomena in plasmas and global magnetic reconnection</b>	<b>150</b>
9.1	Magnetic self-organization in plasmas	150
9.2	Magnetic self-organization in laboratory plasmas	152
9.3	Impulsive self-organization in space and laboratory plasmas	167
9.4	Magnetic self-organization in line-tied magnetic flux ropes: Laboratory study of solar flare eruption phenomena	167

<b>10</b>	<b>Studies of energy conversion and flows in magnetic reconnection</b>	<b>177</b>
10.1	Experimental study of magnetic energy conversion in the reconnection layer in a laboratory plasma	177
10.2	Experimental setup and plasma parameters	179
10.3	Electron flow dynamics studied by measured flow vectors	180
10.4	Observation of energy deposition on electrons and electron heating	181
10.5	Generation of an electric potential well in the two-fluid reconnection layer	184
10.6	Ion acceleration and heating in the two-fluid reconnection layer	187
10.7	Experimental study of the dynamics and the energetics of asymmetric reconnection	190
<b>11</b>	<b>Analysis of energy flow and partitioning in the reconnection layer</b>	<b>198</b>
11.1	Formulation for a quantitative study of energy flow in the reconnection layer	198
11.2	Analysis of energy flow in the two-fluid formulation	201
11.3	Experimental study of the energy inventory in two-fluid analysis	202
11.4	Particle-in-cell simulations for the MRX energetics experiments	205
11.5	A simple analytical model of energy conversion in the two-fluid reconnection layer	208
11.6	Summary and discussions on the energy inventory of the reconnection layer	212
<b>12</b>	<b>Cross-discipline study of the two-fluid dynamics of magnetic reconnection in laboratory and magnetopause plasmas</b>	<b>214</b>
12.1	Background of a collaborative study of two-fluid dynamics in the reconnection layer	214
12.2	Dynamics of the electron diffusion region and energy deposition measured by MRX	217
12.3	Dynamics of the electron diffusion region and energy deposition measured by MMS	218
12.4	Ion dynamics and energetics in MRX and the magnetosphere	222
<b>13</b>	<b>The dynamo and the role of magnetic reconnection</b>	<b>223</b>
13.1	Galactic magnetic fields and basic MHD theory	224
13.2	The Biermann battery dynamo	226
13.3	Research on dynamo effects in laboratory fusion plasmas	227
13.4	Effects of a two-fluid dynamo in an RFP plasma	229
<b>14</b>	<b>Magnetic reconnection in large systems</b>	<b>232</b>
14.1	Development of plasmoid theory	232
14.2	Effects of MHD turbulence on magnetic reconnection	236
14.3	Experimental status of magnetic reconnection research for a large system	240
14.4	Magnetic reconnection in a large system of electron–positron pair plasma	242
14.5	Impulsive reconnection in a large system	243

<b>15 Summary and future prospects</b>	<b>245</b>
15.1 Major findings from local analysis	245
15.2 Major findings from global analysis	247
15.3 Outstanding issues and future research	249
15.4 Closing remarks	250
<b>Appendix A Basic description of waves by dispersion relationship equations</b>	<b>252</b>
A.1 Basic description of waves in cold plasmas	252
A.2 The dispersion relation	254
<b>Appendix B Plasma parameters for typical laboratory and natural plasmas</b>	<b>258</b>
B.1 Plasma parameter diagram	258
B.2 Typical plasma parameters and formulae	258
<b>Appendix C Common notation</b>	<b>260</b>
<b>Bibliography</b>	<b>261</b>
<b>Index</b>	<b>281</b>

# Chapter One

---

---

## Introduction

This monograph describes how our understanding of magnetic reconnection, a fundamental process in the universe, has developed from a classical concept based on magnetohydrodynamics (MHD) to a modern concept based on kinetic and two-fluid physics theory, by which many phenomena observed in laboratory and space plasmas are now explained.

### 1.1 CONCEPT OF MAGNETIC RECONNECTION AND ITS DEVELOPMENT

Magnetic reconnection is a fundamental physical process in which magnetic-field-line configuration changes its topology, leading to a new equilibrium state of lower magnetic energy. During this process, part of the magnetic energy is converted into the kinetic energy of plasma through acceleration or heating of charged particles, which is the most important aspect of magnetic reconnection. In astrophysical and laboratory plasmas, magnetic reconnection occurs ubiquitously, rearranging the configuration of magnetic field lines and simultaneously changing macroscopic quantities of plasmas such as flow and temperature. Magnetic reconnection is seen in the evolution of solar flares, coronal mass ejection, and in the interaction of solar winds with the earth's magnetosphere. It is considered to occur in the formation of stars. It also occurs during the self-organization process of current-carrying fusion plasmas.

In magnetic fusion devices, plasma is confined by the combined forces of internal and external magnetic fields. Thus, the interaction of magnetic field lines with plasma determines the confinement features of hot plasmas. In toroidal fusion devices, toroidal currents are usually induced to heat the plasma and generate magnetic field configurations that effectively confine the hot fusion plasma by compressing pinch forces. There is a remarkable feature common to these configurations: the plasmas constantly tend to relax to a quiescent state through global magnetic self-organization processes in which magnetic reconnection plays a key role. Understanding and controlling magnetic reconnection in fusion devices is essential to creating a reliable fusion reactor core.

Magnetic fields can be found everywhere in the universe at all scales: in the earth's magnetosphere, in the solar corona, and on larger scales from the interstellar medium to galaxy clusters. How are magnetic fields generated in the universe? How do they determine the properties of plasmas? Understanding magnetic reconnection provides

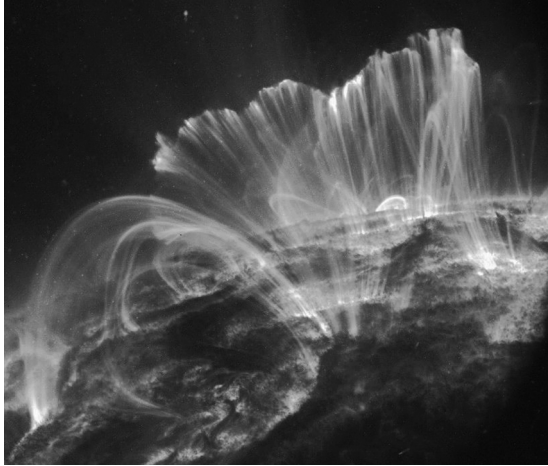


Figure 1.1. See Color Plate 1. Soft-X-ray picture from the TRACE satellite. [<https://www.solar-facts-and-advice.com/solar-flares.html>]

a key to these fundamental questions about the universe. When magnetic energy significantly exceeds the plasma's kinetic or thermal energy, the magnetic energy tends to be converted to kinetic energy through magnetic reconnection. When there is abundant kinetic energy in a plasma with respect to magnetic energy, just like in the early universe ( $W_p \gg W_B$ ), magnetic fields are considered to be generated through a converse process, a dynamo mechanism in plasma. Even in this dynamo process, magnetic reconnection often plays an important role.

Solar flares exhibit perhaps the clearest visual examples of magnetic reconnection and have been investigated for many decades. Through soft-X-ray pictures, which are considered to represent magnetic-field-line configurations of the solar atmosphere, we can visualize illuminating examples of the global topology change of plasma configurations (Tsuneta, 1996; Masuda et al., 1994; Gabriel et al., 1997; Golub et al., 1999; Lin et al., 2003). As shown in TRACE satellite data (Golub et al., 1999; figure 1.1), the topologies of soft-X-ray images are seen to change within a timescale of minutes or hours in the solar atmosphere, in which the magnetic diffusion time for a typical flare, based on the classical calculation for collisional diffusion, is estimated to be as long as 1 million years. These observations suggest the presence of fast changes of the global field-line topology, implying the existence of an anomalously fast magnetic reconnection process. Giovanelli (1946) noted that the abundant magnetic field energy in the chromosphere could be converted to electron kinetic energy during this process. Although the theory of MHD was not used in his calculation and the evolution of the sunspot field was treated as though it was a low-frequency wave, satellite measurements later showed that his concept is indeed valid and can be applied to solar corona reconnection.

In the early days of plasma research, a powerful way of describing the plasma dynamics was developed based on MHD, which treat plasma as a one-fluid element.

MHD theory was built upon the foundation of hydrodynamics by implementing the theory of electromagnetism. This MHD was found to be very effective, particularly when the Lundquist number (which is defined as the ratio of the magnetic diffusion time ( $=\mu_0 L^2 V_A/\eta$ ) to the crossing time of the Alfvén waves ( $=L/V_A$ ) in the region) is high ( $S \gg 1$ ):  $S \sim 10^{12}$  for a solar flare plasma of 10,000 km and  $S > 10^6$  for tokamak plasmas. In this situation, plasma dynamics can be formulated based on the principle of flux freezing, namely that plasma always moves with magnetic field lines (as if it is frozen to them) with no dissipation. We call this principle “ideal MHD” dynamics. In ideal MHD, the plasma resistivity caused by collisions between electrons and ions and the viscosity caused by like-particle collisions are neglected in most cases. On the other hand, it was also realized that ideal MHD breaks down in a region of magnetic reconnection because the flux freezing principle does not hold in reconnecting plasmas. In other words, magnetic reconnection, in which field lines change their topology inducing magnetic energy dissipation at the reconnection layer, cannot be described by ideal MHD.

How do magnetic field lines move around in plasmas and how do they reorganize? Ideal MHD, developed in the early 1950s, describes the dynamics of highly conductive plasmas, where the electric field parallel to the magnetic field line,  $E_{\parallel}$ , vanishes (Sweet, 1958; Parker, 1957; Vasylunas, 1975; Dungey, 1995). In this idealized model, magnetic field lines always move with the plasma and remain intact and never break or tear apart, as we will see in chapter 3 in detail. To consider the physical picture of this situation more precisely, we can represent any magnetic field by a set of lines that fills the system. The lines are tangent to the magnetic field and their density equals the field strength. If the system is time dependent, the features of the lines are different at every instant. If the plasma moving with the field lines is infinitely conducting, a physical identity can be assigned to the lines. If the magnetic field lines move with the plasma, they will continue to represent the magnetic field at any later time. This allows us to picture the magnetic field clearly. The field thus consists of strings embedded in the plasma which are neither created or destroyed. The magnetic force is represented by imagining the strings to have longitudinal tension and transverse pressure. If the strings are sharply bent, the curvature force replicates the magnetic tension force. If the lines are put closer together and bunched in a region, there is a transverse force due to the magnetic pressure force. Any plasma on a given line stays on that line as it moves, and cannot move to another line. This is basically the flux freezing feature associated with ideal MHD. We will revisit this concept later in detail in chapter 3.

Let’s consider two magnetic field lines that are approaching each other in a small region of plasma. Outside this region, plasma fluid is frozen to field lines as described by ideal MHD. When the two field lines approach very close at an angle in a narrow region (figure 1.2), the magnetic field gradient becomes large. This interaction of magnetic field lines generates a current sheet due to Ampère’s law  $\nabla \times \mathbf{B} = \mu_0 \mathbf{j}$ . We note that since the presence of a current sheet requires different motions of electrons and ions, strictly speaking this phenomenon cannot be described by single-fluid ideal MHD theory. The exact treatment of this region requires two-fluid physics as described in chapters 4 and 5. In MHD theory, we called this a diffusion region. In this area, the field lines are not frozen to the plasma, and they lose their identity, break, and reconnect.

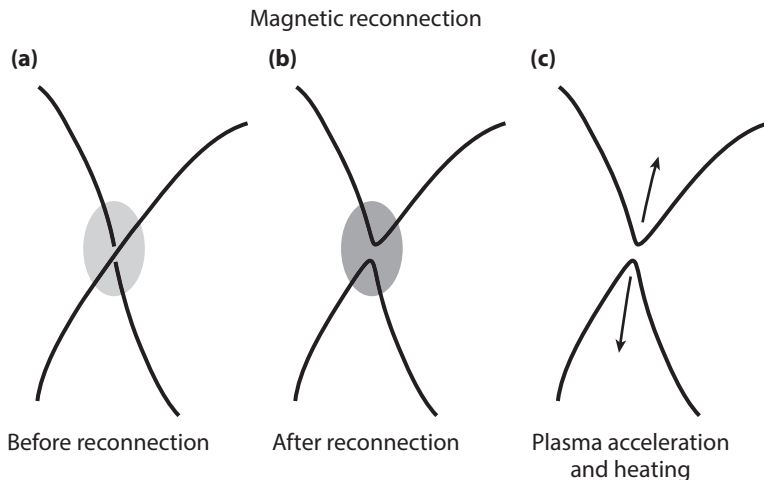


Figure 1.2. Schematic view of magnetic reconnection. After reconnection, plasma heating and acceleration follow.

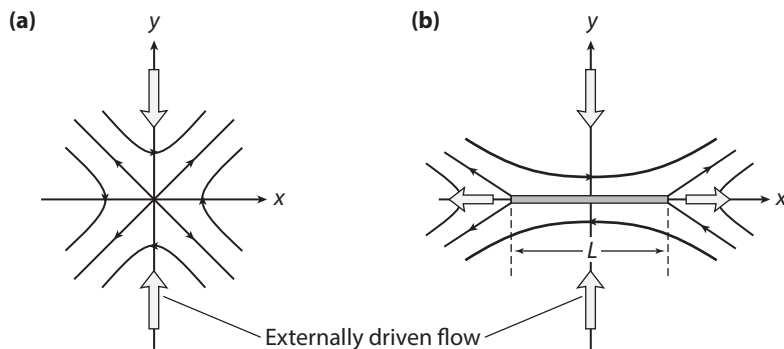


Figure 1.3. Formation of current sheet by externally driven flow. [From Biskamp (2000).]

After reconnection occurs, the two newly connected field lines accelerate plasma fluid due to a tension force generated by the reconnection. This interaction of field lines leads in most cases to a singular sheet of high current density in plasma where  $E_{\parallel}$  becomes sufficiently large ( $E_{\parallel} = \mathbf{E} \cdot \mathbf{B} / B \neq 0$ ) to induce nonideal-MHD plasma behavior and to cause the magnetic field lines to lose their connectivity and identity. This is why we call it a diffusion region.

As shown in two-dimensional geometry by figure 1.3, Dungey (1953) showed that such a current sheet can indeed be formed in a plasma by the collapse of the magnetic field near an X-type neutral point, and suggested that “lines of force can be broken and rejoined in the current sheet.” We note that if it were not for a plasma, this would



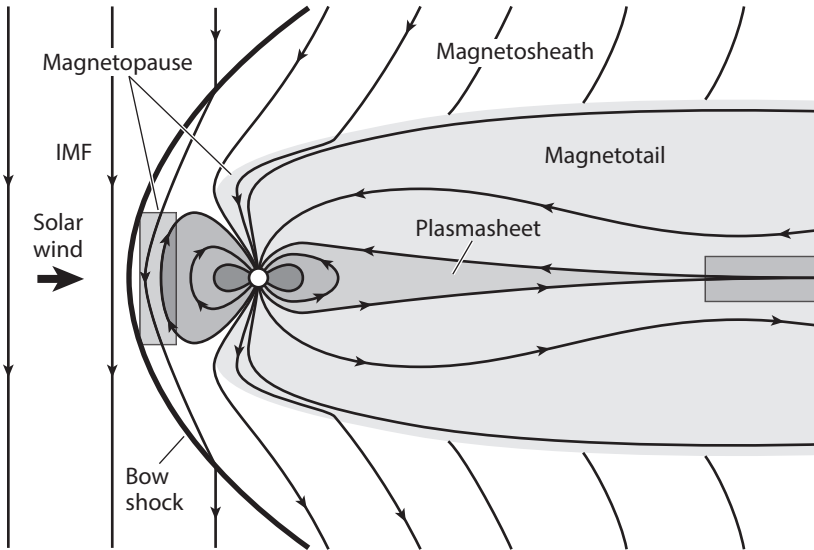


Figure 1.4. Cross-section of the simplest model of the magnetosphere in the day and night meridian. [From <https://mms.gsfc.nasa.gov/science.html>.]

not happen. Instead, the two opposing field lines would meet with an X-type crossing of angle 90 degrees, satisfying the Maxwell equations in a vacuum,  $\nabla \times \mathbf{B} = 0$  (because there is no current sheet) and  $\nabla \cdot \mathbf{B} = 0$ . This sheet in a plasma is called a neutral sheet or a current sheet. As previously mentioned, it is often called a diffusion region since magnetic field lines lose their connectivity, diffuse, and reconnect in the sheet. When the field lines are reconnected, the topology of magnetic configuration changes and  $\mathbf{j} \times \mathbf{B}$  forces expel the plasma from the diffusion region and result in the conversion of magnetic energy into kinetic energy. Thus, it is important to note that while the topology of magnetic configurations changes by magnetic reconnection, the conversion of magnetic energy to kinetic energy occurs at the same time and the plasma gains energy. This is a very important aspect of magnetic reconnection, as mentioned before.

An important example of flux freezing and magnetic reconnection in a space plasma is shown in figure 1.4, illustrating a simplified two-dimensional schematic picture of the solar-wind interaction with the earth's magnetosphere. The plasma on the incoming solar wind is embedded on solar-wind magnetic field lines that are separated from the magnetospheric lines. In the ideal MHD picture, there is no way for the solar-wind plasma and energetic particles to penetrate into the earth's magnetosphere, owing to the flux freezing principle. The solar wind is accordingly forced to move around the magnetosphere and is blown downstream.

At the magnetopause, where the solar wind presses against the magnetic pressure of the earth's dipole field, the interacting region becomes very thin, and the motions of

plasma particles, ions, and electrons are quite different with respect to the magnetic fields of both sides and in the thin magnetic reconnection region. To describe this type of reconnection layer, a more general theory than MHD is necessary for a proper treatment of the neutral layer, that takes into account the different behaviors of electrons and ions. Reconnection layers, such as those created in the magnetopause (Vasyliunas, 1975; Dungey, 1995; Kivelson and Russell, 1995), have thicknesses that are comparable to the ion skin depth  $c/\omega_{pi}$  ( $\sim 50$  km). This situation leads to strong two-fluid effects, especially the Hall effect, in which magnetized electrons flow perpendicular to the magnetic fields in the neutral sheet. This effect induces a large reconnection electric field at the reconnection region and is thus considered to be responsible for speeding up the rate of reconnection, which is larger than the classical MHD rate (to be described in chapter 5).

In such a situation, magnetic reconnection takes place at the front and the tail parts of the magnetosphere, even if the plasma is truly infinitely conducting. Because of magnetic reconnection, some of the solar-wind lines break near the surface separating them and they reconnect to lines in the magnetosphere, which also break. As a result, some of the solar-wind lines end up attached to the magnetosphere, allowing the solar-wind plasma to penetrate the magnetosphere. This process can be regarded as the converse of flux freezing because of flux dissipation. Solar cosmic rays can also get into the magnetosphere because of magnetic topology changes and are often measured.

How such physical processes occur and how fast line breaking takes place have been the subjects of research for more than a half century. Thanks to recent collaborative research using observations, experiments, and numerical and theoretical works, significant progress has been made in understanding magnetic reconnection. Early work based on elementary MHD physics demonstrated the possibility of reconnection, but predicted reconnection rates that are too slow to explain the observations. As a result of the application of more advanced physics that take into account two-fluid physics and the kinetic effects of plasma particles, much insight has been obtained, and the reasons why reconnection is so much faster than first theorized have become clearer. It is essentially a partial breakdown of the remarkable property of flux freezing described by ideal MHD.

Thus, magnetic reconnection in the magnetosphere is treated using the two-fluid theory. It should be noted, however, that the flux freezing concept can still be applied in a modified form to the two-fluid regime in which electrons are still magnetized but ions are not. In this regime, magnetized electrons move with field lines for the most part, as if the flux freezing principle works only for electron fluid. On the other hand, ions are generally not magnetized and the different motions of electrons and ions can generate electric field in the reconnection plane. They also induce a large Hall electric field in the out-of-reconnection plane and as a result cause a fast reconnection as described in chapter 5. The induced electric fields introduce a new strong mechanism of particle acceleration and heating. This regime is sometimes called the electron-MHD regime. The region in the center of the reconnection layer, where even electrons do not move with field lines anymore and diffuse, is called the electron diffusion region. A good part of this monograph is devoted to a description of the key dynamics of this unique reconnection region.

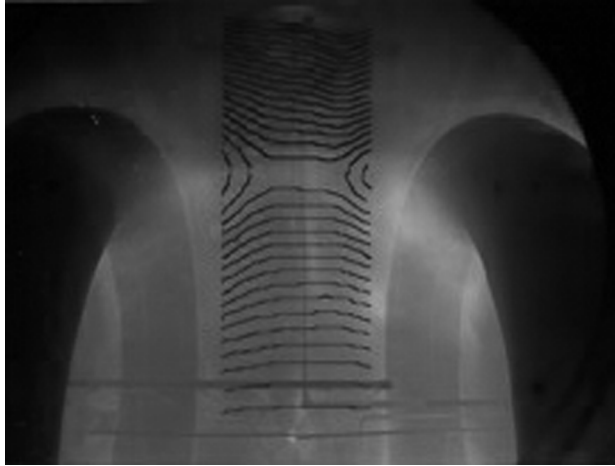


Figure 1.5. See Color Plate 1. Picture (time integrated) of controlled driven reconnection discharges in MRX and a flux plot from magnetic probes from an MRX movie. The flux contours deduced by assuming toroidal symmetry are considered to represent magnetic field lines without guide field. [<https://mrx.pppl.gov/mrxmovies/Collisional.mov>]

## 1.2 RECENT DEVELOPMENT AND PROGRESS OF UNDERSTANDING MAGNETIC RECONNECTION

Progress in understanding the physics of magnetic reconnection has been made in three research fields of the discipline in the past several decades: space and astrophysical observations, theory and numerical simulations, and laboratory plasma experiments. Space and astrophysical observations have provided much key suggestive evidence that magnetic reconnection plays an important role in natural plasmas and have generated strong motivation for fundamental research. Theory and numerical simulations provide important analysis and insights to help break down the complex reconnection phenomena into a set of fundamental key processes and to gain understanding of each process. Magnetic fusion plasma experiments provide examples of magnetic reconnection through self-organization of the plasma configurations. Laboratory experiments dedicated to the study of the fundamental reconnection physics can measure quantitatively the characteristics of reconnection dynamics by monitoring the essential plasma parameters simultaneously at a large number of points in the reconnection region (Yamada et al., 2010).

Figure 1.5 presents an example of contours of magnetic flux which were deduced from experimentally measured data using internal magnetic probes located at multiple locations in the reconnection region of the Magnetic Reconnection Experiment (MRX; Yamada et al., 1997a; Yamada, 1999). Dedicated laboratory experiments quantitatively cross-check theoretically proposed physics mechanisms and models, and provide a bridge between space observations and theoretical ideas, such as two-dimensional two-fluid reconnection models, by generating a typical reconnection layer. On the other

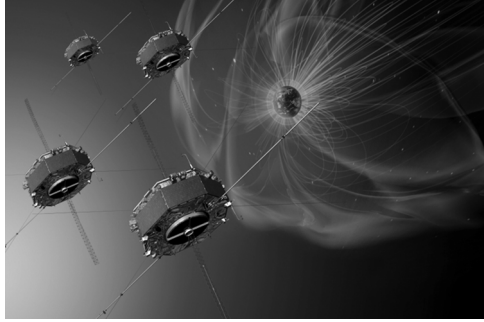


Figure 1.6. MMS satellite mission. Four satellites measure key components of local plasma parameters to document the electron and ion dynamics. [From [https://en.wikipedia.org/wiki/Magnetospheric\\_Multiscale\\_Mission](https://en.wikipedia.org/wiki/Magnetospheric_Multiscale_Mission).]

hand, space satellites can provide detailed data at selected points with simultaneous multiple sophisticated diagnostics. Recent significant progress in data acquisition technologies has allowed us to directly compare the observed data from satellites and laboratory experiments recently published (Yamada et al., 2018). In laboratory experiments, even an evolution of magnetic field lines was able to be monitored with respect to time. Remarkably, through this cross-cutting research, a new common picture of the two-fluid magnetic reconnection layer has emerged, aided by numerical simulations mostly performed in two-dimensional geometry. We use a significant part of this monograph to describe the two-fluid physics mechanisms that have become clearer through our cross-discipline studies.

In particular, a new cluster satellite system, called the Magnetospheric Multiscale Satellite (MMS) was launched in March 2015. Their mission goal was to explore the physics of magnetic reconnection in spatial scales extending down to the thin electron skin depth. Figure 1.6 shows a graphic picture of four satellites that measure key components of local plasma parameters to document the electron and ion dynamics. The four spacecraft are placed at times in a tetrahedral configuration with a separation of about 7–10 km, or  $\sim 3$ –5 times the expected value of the electron skin depth at the magnetopause. Since the current sheet moves past the spacecraft at speeds of over 100 km/s, resolving these fine-scale structures requires field measurements at a 1 ms cadence and particle distribution function measurements at a 20 ms cadence, which is challenging for a spacecraft mission.

To date, the MMS mission has made many significant findings, identifying the structure and the dynamics of the electron diffusion region both in the magnetopause and the magnetotail reconnection layer. In the first phase of the MMS mission, the dayside magnetosphere reconnection region was investigated. At the subsolar magnetopause, where the solar-wind plasma meets the magnetospheric plasma, reconnection is very asymmetric with an upstream plasma density larger than that of the magnetosphere by a factor of 10–20. Subsequently, the magnetic field strength is smaller by a factor of 2 to 3. This asymmetric reconnection is of much interest and is often very important for real physical situations in both space and astrophysical plasmas (Mozer

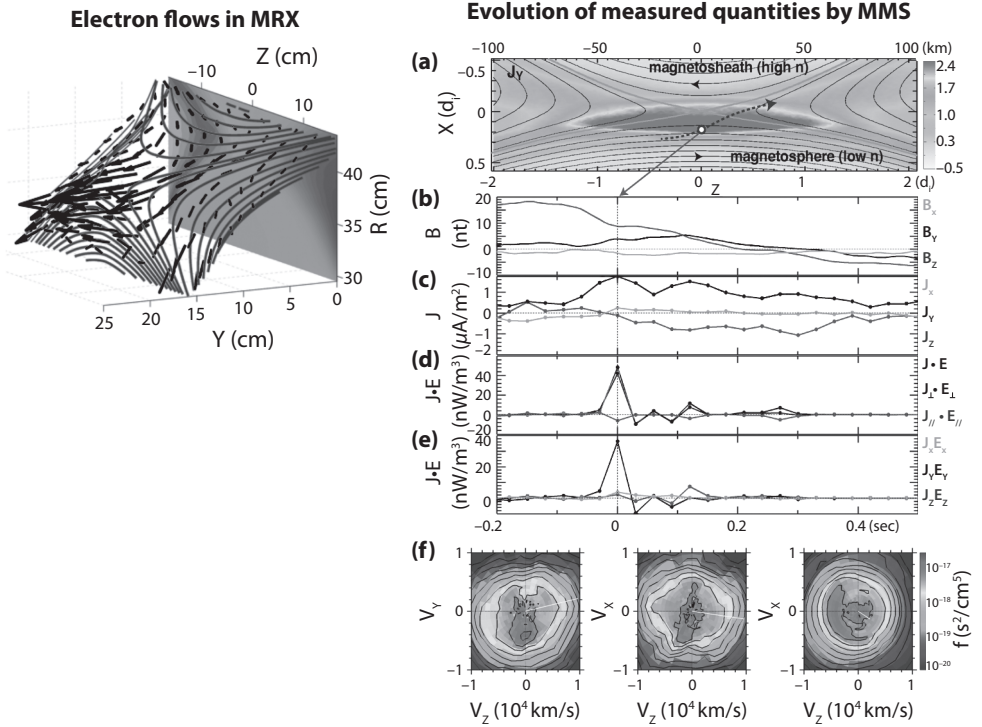


Figure 1.7. See Color Plate 1. Comparison of MRX and MMS data. Left: Measured electron flow vectors in MRX (red arrows). Measured magnetic flux contours are shown by blue lines. Right: (a) Approximate MMS trajectory through the electron diffusion region of the magnetosphere. The trajectory is determined based on a comparative study of MMS data and 2D numerical studies. (b)–(f) Time evolution of key components of local plasma parameters showing that  $\mathbf{J}_\perp \cdot \mathbf{E}_\perp$  becomes maximum at the electron diffusion region (d). The electron velocity distributions in (f) show that they predominantly flow in the  $Y$ -direction as shown in the MRX data. The documented MMS data are remarkably consistent with the electron dynamics measured by MRX. [From Yamada et al. (2018).]

and Pritchett, 2011). Recently, through a collaboration between MMS research and MRX, the key physics of asymmetric reconnection have been intensively investigated and illuminated (Yoo et al., 2017; Yamada et al., 2018).

Both in MRX and in the magnetopause plasmas, the length of the reconnection layer was measured to be very similar, about 3 times the ion skin depth, indicating the same physics mechanisms are at play. Taking advantage of this situation, the dynamics and energetics of the magnetic reconnection layer were comparatively studied in the context of two-fluid physics. Despite huge differences between the length scales of the reconnection layers ( $2L \sim 30$  cm in MRX versus  $\sim 250$  km in the magnetopause)

and the ion skin depths ( $d_i \sim 5\text{--}6\text{ cm}$  in MRX versus  $\sim 50\text{ km}$  in the magnetopause), remarkably similar characteristics are observed regarding the dynamics of electrons and ions, as well as energy deposition profiles and energy partitioning. Let us look into common characteristics observed in MRX and MMS.

Figure 1.7 shows a comparison of MRX and MMS data sets in different formats. Electron flow vectors (red arrows) measured in MRX show strong out-of-reconnection-plane electron flows. Also, a strong energy deposition to electrons is measured to occur through a large value of the  $\mathbf{j}_e \cdot \mathbf{E}$  quantity (Yamada et al., 2014) in MRX. Here it should be noted that the uppercase letter  $J$  was used for electron current density in the MMS data set, while lowercase  $j$  was used in the MRX data as well as in most of this book. On the right, panels (a)–(f) show the time evolution of key components of local plasma parameters, documenting the electron dynamics in the magnetopause. These MMS data show a strong spike in the quantity  $\mathbf{j}_e \cdot \mathbf{E}$  when the satellite system flies through the region just south of the X-point where reconnecting field lines meet and reconnect. This observation is in remarkable agreement with the profile of electron flow vectors measured on MRX as seen in the left-hand panel of figure 1.7. When the energy deposition rate to electrons,  $\mathbf{j}_e \cdot \mathbf{E}$ , is decomposed into  $\mathbf{j}_{e\perp} \cdot \mathbf{E}_\perp + j_{e\parallel} E_\parallel$ , i.e., separating the inner product into perpendicular and parallel components with respect to the local magnetic field lines,  $\mathbf{j}_{e\perp} \cdot \mathbf{E}_\perp$  is measured to be significantly larger than  $j_{e\parallel} E_\parallel$  as shown in panel (d) of figure 1.7. In addition, the measured electron velocity distributions in the three directions are consistent with the MRX data of electron flow vectors shown on the left.

Further observational verifications of electrons' motion frozen to field lines outside the electron diffusion region were made both in MRX (Yoo et al., 2013) and MMS (Burch et al., 2016b), and excellent agreement was found between the dynamics and energetics of electrons. This agreement demonstrates that the same two-fluid mechanisms in two-dimensional analysis operate well in both systems, despite vastly different scales ( $\sim 10^6$ ), while various three-dimensional phenomena including micro-fluctuations are expected to be involved. This will be discussed in more detail in chapter 12.

### 1.3 MAJOR QUESTIONS

We address the following major questions, which have been studied intensively for the past 30 years:

- (1) Why is the reconnection rate so fast in collisionless conductive plasmas? What is a scaling for the reconnection rate on collisionality?
- (2) What are the mechanisms of magnetic reconnection in collisionless plasma? How does two-fluid physics influence the dynamics and speed of local reconnection? What determines the structure of the reconnection layer?
- (3) How is magnetic energy converted to the kinetic energy of electrons and ion? In what channel does the energy flow take place?

- (4) How do fluctuations and turbulence affect the reconnection dynamics or vice versa? Which fluctuations are most relevant, how are they excited, and how do they determine the reconnection rate and influence the conversion of magnetic energy?
- (5) How do reconnection features change as the size of the plasma system increases? How are plasmoid structures formed and how do they influence the reconnection rate?
- (6) How is the local physics, which has been studied in great detail, connected to the large global environment around the reconnection layer? How is the reconnection layer generated in a global boundary of different sizes?
- (7) Why does reconnection occur impulsively in most cases?

Keeping these questions in mind, we will study most of the significant modern experimental findings and discoveries in magnetic reconnection research and discuss many of the theoretical understandings to which they have led.

To begin, we review magnetic reconnection research and significant studies that have continued up to the present time, beginning with the well-known seminal ideas of Dungey, Sweet and Parker, and Petschek, based on MHD. While theory led the early research progress in this area, more recent research has been dominated by experiments and numerical simulations. Since the early work is fairly well known and presented in textbooks, we focus on recent findings and developments of most significance. There are a number of different views as to which physical processes are most important for reconnection. While the relative importance of two-fluid processes of a laminar current sheet versus three-dimensional fluctuation-induced effects of multiple reconnection sites or plasmoids are still debated, our goal is to provide a broad understanding of different theories and observations.

One of the most important questions has been why reconnection occurs much faster than predicted by classical MHD theory. During the past two dozen years, notable progress in understanding the physics of this fast reconnection has been made. Extensive theoretical and experimental work has established that two-fluid effects, resulting from the fundamentally different behavior of ions and electrons, are important within the critical layer where reconnection takes place. Two-fluid effects are considered to facilitate the fast rate at which reconnection occurs in the magnetosphere, stellar flares, and laboratory plasmas. Dedicated laboratory experiments and magnetospheric satellite measurements show strikingly similar data in the profiles of magnetic fields and electrostatic and magnetic fluctuations. Recent improvements in the understanding of the role of reconnection in magnetic self-organization processes in laboratory and space-terrestrial plasmas will also be covered in this monograph.

Despite the long history of reconnection research, how the conversion of magnetic energy occurs remains a major unresolved problem in plasma physics. A good amount of the recent studies on energy conversion are presented in the present monograph. In the past several years, it has been realized that energy conversion in a laboratory reconnection layer occurs in a much wider region than previously considered. The mechanisms for energizing plasma particles in the reconnection layer are identified, and a quantitative inventory of the converted energy is presented for the first time in

a well-defined reconnection layer in a laboratory plasma study (Yamada et al., 2014, 2018). In this monograph, a new analytical study is considered for a key step toward resolving one of the most important problems in reconnection physics.

A special effort is made to cover both the major experimental results and recent space observations that have provided useful information on the physics of magnetic reconnection over the past few decades. This book is quite different in emphasis from recent review papers and books, which have emphasized theoretical aspects or results from numerical simulations. Since the main objective of this book is not a review, many fine works in this field are not covered because of space limitations, because of our primary focus on recent experimental findings, and because of our intention to convey my views to the readers.

Magnetic reconnection is a very popular subject in plasma physics. For some years, the numbers of papers submitted to annual meetings of the Division of Plasma Physics of the American Physical Society (APS) have exceeded 100 (out of 1,500–1,800 total papers). To cover wider aspects of the physics of magnetic reconnection, I would like to refer to the books by Priest and Forbes (2000), Biskamp (2000), Birm and Priest (2007), the reviews Zweibel and Yamada (2009), Yamada et al. (2010), and the collection of edited reviews in Gonzalez and Parker (2016). Magnetic reconnection research covers plasmas of many types, including weakly ionized, electron–positron pairs, and relativistic plasmas. The reader seeking special material should consult additional references including Uzdensky (2011) for reconnection in relativistic or astrophysical environments and Ji et al. (2022) for recent development of reconnection research in large systems.

An important perspective is that magnetic reconnection is influenced and determined both by local plasma dynamics in the reconnection region and global boundary conditions. One major question is how large-scale systems generate local reconnection structures through formation of current sheets—either spontaneously or via imposed boundary conditions. In this regard, we will look into the question of how multiple reconnection layers are formed in a large plasma system. When we consider a large system in which reconnection takes place, we think all classical models do not simply apply, particularly when long global lengths are assumed for the current layers. Recently, more research has been carried out on the formation process of current layers in a larger system and has found that a current sheet often breaks up to form multiple reconnection layers. It would be of great importance to develop and elucidate a general theory of current layer formation in a highly nonsymmetric magnetic equilibrium such as is observed in the magnetopause or the sun. We will address magnetic reconnection in the magnetopause where strong density asymmetry exists across the reconnection layer. There may be mechanisms to generate multiple small-scale current sheets in which field-line reconnection takes place with multiple X-lines. These structures can often be small enough to decouple the motion of electrons from that of ions in collisionless plasmas. These smaller-scale sheets can fluctuate, leading to faster reconnection, and a large number of these layers should lead to a large energy release as seen, for example, in the magnetosphere and the reversed field pinch (RFP) plasmas for fusion research. In RFP plasmas, reconnection in multiple layers of flux surfaces is observed to generate a significant magnetic self-organization of the global plasma, invoking strong ion heating. While we expect that a theory from a first principle can



lead us to a breakthrough for solving this problem, we have recently initiated a new experimental effort to address this important issue (see chapter 14).

In this monograph, we describe the fundamental physics of magnetic reconnection at work in laboratory and space plasmas, starting from concept, theory, and observations from space satellites, and also the most important progress in the research fronts. With a brief review of the well-known work on its concept, together with the most recent results in chapter 1, typical reconnection phenomena observed in space and laboratory plasmas are presented in chapter 2, and important theoretical progress based on MHD is described in chapter 3. A one-dimensional Harris sheet equilibrium with kinetic physics is studied in chapter 4, referring to both early theoretical and experimental results. In the area of local reconnection physics, many findings have been made regarding two-fluid physics analysis and are related to the cause of fast reconnection. Chapter 5 describes the evolution of two-fluid physics and formulation. Profiles of the reconnection layer, Hall currents, and the effects of a guide field, collisions, and microturbulence are discussed in chapter 5 to understand the fundamental processes in reconnection layers in both space and laboratory plasmas. In chapter 6, the primary laboratory experiments of past and present times are described.

Chapters 7 and 8 are devoted to observation of magnetic reconnection in astrophysical plasmas, in particular reconnection in solar flares, coronal mass ejection, reconnection in the Crab Nebula or supernova, and the dynamics of the magnetic reconnection layer in the magnetosphere. Some readers may find chapter 8 to be too detailed and hard to follow since I use specific wording and descriptions used in the space physics community. Chapter 9 is devoted to magnetic self-organization in laboratory plasmas or global reconnection phenomena. In chapter 10, we address extensively the energy flow processes and present the mechanisms of energy conversion and partitioning, which have been discovered in the recent few years. Furthermore, more accurate recent satellite observations will be presented regarding magnetic reconnection and its energetics in space astrophysical plasmas and those will also be covered in this book. Chapter 11 covers the most recent studies of the energy inventory in the reconnection layer. In chapter 12, let us directly compare the dynamics and energetics of the asymmetric reconnection layer observed both in the laboratory plasma of MRX and in the magnetopause by MMS and discuss our results in the context of two-fluid physics, aided by simulations. In chapter 13 we consider how magnetic field is generated in the universe and how magnetic reconnection plays a role in the dynamo. Since the focus of this monograph is two-fluid physics mechanisms, we mainly consider here the two-fluid effects of dynamo action in fusion laboratory plasmas, after a brief introduction to MHD dynamo theory. In chapter 14 we consider magnetic reconnection in large systems. In astrophysical plasmas, the ratio of global to kinetic scales is large and the ratio of mean free path to plasma scales is small, thus MHD models are often considered to be practical to treat space astrophysical phenomena. The appearance of multiple layers would become dominant, particularly in large three-dimensional plasma systems. Readers who might find it difficult to follow the detailed technical description of results in some chapters, such as 8 and 9, might be recommended to skip them and move on in order to grasp the whole picture of magnetic reconnection.

---

---

## Index

- ACE satellite, 52, 53–54
- Alfvén waves: concepts of magnetic reconnection and, 3; dispersion and, 257; dynamos and, 228; energy flows and, 177–78, 199, 201, 212; impulsive occurrence of, 128; kinetic theory and, 59–60; laboratory plasmas and, 98, 101, 106, 168, 173–74, 259; large systems and, 237–38; magneto-hydrodynamics (MHD) theories and, 40–44; magnetotail and, 148; self-organization and, 168, 173–74; solar flares and, 17, 19–20, 127–30; Sweet-Parker model and, 40–42; transit times of, 101; two-fluid theory and, 65, 87, 90, 215, 219
- American Physical Society, 12
- Ampère’s law, 3, 21, 32, 75, 136
- asymmetric reconnection: dynamics/energetics of, 190–97, 213; field strength and, 8; magnetopause and, 142, 148; merging and, 109; MMS/MRX collaboration and, 9, 13; two-fluid effects and, 86, 96, 214–18, 222
- astrophysical jets: chromospheric, 123–30; collimated, 115, 116, 227; CSHKP model and, 17; electron-positron plasma and, 242; energy flows and, 202; high- $\beta$  plasmas and, 115; low altitude coranae and, 18–20; magnetopause and, 138–43; magnetotail and, 146–48; recent observations on, 15; X-line and, 54; X-ray, 18–19, 123–25, 127
- astrophysical plasmas: acceleration and, 130–33; collisions and, 132–34; concepts of magnetic reconnection and, 1, 7–8, 12; Crab Nebula and, xii, 13, 130–33, 243; dynamos and, 223, 225, 227; electron diffusion region (EDR) and, 137; energy flows and, 13, 200–201, 205; field lines and, 130, 132; FLARE and, 113, 115; future research and, 249; guide field and, 134; Hall effect and, 134; heating and, 134; ions and, 132–34; kinetic theory and, 134; laboratory plasmas and, 130, 134; large systems and, 232, 236, 240–43; magnetopause and, 135–46; magnetotail and, 146–49; merging and, 130, 132; MRX and, 109, 131; neutral sheets and, 133, 134; particle-in-cell (PIC) simulations and, 130; Petschek model and, 44; reconnection layer and, 130, 132–34; scaling data and, 94–96; self-organization and, 150, 152; solar flares and, 20, 131, 133–34; spheromak plasmas and, 131; thermal energy and, 132; X-lines and, 134; X-point and, 134; X-rays and, 131

- Bateman, G., 20  
Bhattacharjee, A., 69, 72, 164, 235  
Biermann battery dynamo, 226–27  
Big Bang, 223  
Birdsall, C., 68  
Biskamp, D., 44–45  
breakout model, 123–27
- Carmichael, H., 118  
Carmichael-Sturrock-Hirayama-Kopp-Pneuman (CSHKP) model, 15–17, 121–23  
Carrington, R. C., 117  
Cassak, P., 219, 235  
Center for Magnetic Self-Organization (CMSO), 251  
Chapman, S. C., 69  
chromosphere jets, 123–24  
Clebsch coordinates, 35  
Cluster satellite, 52, 53–54, 62–63, 93, 184–86  
collisionless reconnection, 245;  
  energy flows and, 178, 187, 191, 198–99; kinetic theory and, 55, 61, 63, 238; limitation of MHD models and, 129; magnetopause and, 140; magnetotail and, 148; notes on fast, 133–34; Ohm’s law and, 78; two-dimensional numerical simulations for, 69–77; two-fluid effects and, 65, 69–82, 89, 97, 140; X-point and, 242  
connectivity, 4–5, 14, 136, 238  
conversion of magnetic energy, 5, 11, 14, 30–31, 38, 72, 83, 115, 177–78, 198, 246  
coronal heating, 14–15, 19–20, 30, 119, 123–24, 134  
coronal mass ejections (CMEs): chromosphere jets and, 123–24; equilibrium and, 15–16, 20; laboratory plasmas and, 151, 167–70, 169; large systems and, 243; magnetohydrodynamics (MHD) theories and, 53; major findings and, 247; new interpretation of, 124–25; solar flares and, xi, 1, 13–17, 20, 117, 119, 120, 123–25, 126, 129, 247–48; standard model for, 121–23  
cosmic rays, 6, 224  
Coulomb interactions, 68, 78–79, 111, 180, 188, 217, 242  
Cowling, T. G., 224  
Crab Nebula, xii, 13, 130–33, 243  
current sheet: *Color Plate 2*; collapse of, 100; concepts of magnetic reconnection and, 5, 8, 11–12; dynamos and, 227; effective resistivity and, 47–50 (*see also* resistivity); energy flows and, 179, 181, 185–87, 188, 191–92, 202, 208–13; flux ropes and, *Color Plate 8*, 240; global reconnection phenomena and, 165–66; heliospheric (HCS), 130; kinetic theory and, 56–58, 61–63; laboratory plasmas and, 28, 98–101, 111, 114, 116, 150, 152, 156, 165, 172–74; large systems and, 232–35, 238, 240–42; magnetohydrodynamics (MHD) theories and, 31, 38, 42, 47–54; magnetosphere and, 21–22, 136–37, 141, 146–48; major findings and, 247–48; plasmoid theory and, 233; self-organization and, 150, 152, 156, 165, 172–74; solar plasmas and, 16, 118–22, 125–32; Sweet-Parker model and, *Color Plate 3*, 11, 31, 41–46, 55–56, 63, 83, 165, 232–35, 238, 240, 242; two-fluid theory and, *Color Plate 3*, 79–84, 90–94, 97, 214, 216. *See also* neutral sheets
- Daughton, W., 69, 73, 90, 238, 242–43  
Dawson, J., 68  
dayside reconnection, 51  
Debye length, 58, 66

- De Pontieu, B., 19
- diamagnetic (effects), 56, 63, 86, 108, 163, 230
- diffusion region: collisional, 2–3, 23, 47, 65–66, 77–78, 80, 82, 87–89, 93, 96–97, 113, 129, 138–39, 148, 178, 189, 190, 238; electron diffusion region (EDR) and, 6–10, 23, 72, 76–80, 85, 86–88, 94, 96, 137, 139, 146, 178, 181, 183–84, 191, 194–96, 199, 203, 214–22, 238, 246, 250; energy flows and, 177–84, 189–91, 194–96, 199–203, 208, 212; ion diffusion region (IDR) and, 77–80, 84–88, 137–39, 142, 148, 178, 181, 182, 189, 190, 194, 199, 202–3, 208, 211–13, 217–19, 222, 238; magnetohydrodynamics (MHD) theories and, 30, 37–40, 47–48; magnetopause and, 137, 138–43; magnetotail and, 146–48; neutral sheets and, 5 (*see also* neutral sheets); two-fluid effects and, 65–66, 72, 76–89, 93–97, 214–15, 217–22
- dispersion: acceleration and, 257; Alfvén waves and, 257; basic wave description and, 252–54; Fourier analysis and, 252–54; ions and, 257; magnetosphere and, 257; Maxwell’s equations and, 252, 254; MKSA units and, 252, 258; MRX and, 257; Ohmic dissipation and, 183; plasma density and, 257; reconnection layer and, 257; relation of, 254–57; thermal energy and, 257; two-fluid theory and, 72, 89–91; wave description and, 252–57; whistler waves and, 72
- dissipation of magnetic energy, 72, 242
- Drake, J. F., 69, 73, 93, 178
- Dungey, J., 4, 11, 22–23, 28, 31, 38, 41, 46, 98, 100
- dynamoes: Biermann battery, 226–27; dynamo effects in laboratory fusion plasmas, 227–31; Lundquist number and, 228; mean field theory and, 223–25, 228–29
- electron diffusion region (EDR): astrophysical plasmas and, 137; asymmetric reconnection layer and, 194–96; concepts of magnetic reconnection and, 6–10; energy deposition and, 194–96, 211–12, 217–22; energy flows and, 178, 181–84, 191, 194–96, 199, 203; future research and, 250; large systems and, 238, 246; magnetosphere and, 23, 137, 139, 146, 148; major findings and, 246; MMS measurement of, 148–49, 218–22; MRX measurement of, 148, 217–18, 250; two-fluid theory and, 72, 76–80, 85, 86–88, 94, 96–97, 214–22
- electron energization: astrophysical plasmas and, 130–32; energy flows and, 177, 205, 211–13; magnetic islands and, 17; magnetopause and, 145; photosphere and, 84, 123
- electron MHD (EMHD), 6, 93, 101–2, 114
- electron-positron pairs, 12, 17, 131, 132, 242–43, 249
- electron pressure: dynamoes and, 230; Hall effect and, 246; laboratory plasmas and, 101, 113, 116; two-fluid theory and, 73, 75, 78, 83, 96
- energetics of reconnection, 9, 13, 190–97, 214–15, 246
- energy conversion, 11; astrophysical plasmas and, 134; energy flows and, 177–80, 198–212; field lines and, 31; magnetotail and, 148; partitioning and, 13, 198, 214, 247, 249; resistivity and, 42; two-fluid effects and, 72, 214–15, 218–19

- energy flows: guide field and, 194–95, 202, 213; Hall effect and, 178, 181, 184–85, 193–94, 203–5, 212–13; Harris equilibrium and, 205–10; Lundquist number and, 177, 199; Magnetosphere Multiscale Satellite (MMS) and, 181, 190, 194–95; Petschek model and, 178
- energy partitioning, 10, 178, 202, 214
- Facility for Laboratory Reconnection Experiments (FLARE), 113–15
- Facility of Large Reconnection Experiment (FLARE), 241–42
- Faraday's induction, 32
- fast particles, 140, 141
- fast reconnection: energy flows and, 181, 212; Hall effect and, 6, 13, 69, 71–72, 76–77, 84, 86, 96, 134, 181, 212–14, 243; laboratory plasmas and, 99, 103, 116, 151, 157, 167; large systems and, 232–34, 238, 240, 243; magnetohydrodynamics (MHD) theories and, 31, 44, 46–47; major findings in, 245, 247–48, 250; progress in understanding, 11; reversed field pinch (RFP) and, 12; self-organization and, 151, 157, 167; solar plasmas and, 15, 123, 128; two-fluid theory and, 13, 69, 72, 84, 91, 96, 214
- Fermi Gamma-Ray Space Telescope, 130
- field-line topologies, 2, 130, 165, 166
- field reversed configuration (FRC) plasmas, 103, 107–9
- flow vectors: electron, 180–81, 195, 216, 218; flow vectors and, 9, 10, 80, 141, 179, 180–83; ions and, 187–88, 189, 217, 221, 226; MRX and, 9, 10, 80, 141, 179, 180–83, 192, 195, 216
- flux freezing: breakdown of, 37–38; Clebsch coordinates and, 35; concepts of magnetic reconnection and, 3, 5–6; dynamos and, 226; electron fluid and, 78–79; energy flows and, 194, 210; magnetohydrodynamics (MHD) theories and, 33–38; magnetopause and, 144–45; maintaining equilibrium and, 33–37; major findings and, 246; Maxwell's equations and, 37; Ohm's law and, 34, 37; principle of, 33–37; solar plasmas and, 117; Stoke's vector relationship and, 35; two-fluid theory and, 75, 78–79, 219
- Flux Gate magnetometers, 219
- flux ropes: current sheet and, *Color Plate 8*, 240; findings on stability of, 170–72; future research and, 249–50; large systems and, 233, 238–43; Lorentz force and, 68–69, 121, 168, 184; MRX and, 20, 168–72, 238, 242–43; self-organization in line-tied, 167–76; solar flares and, 16, 20, 120–22, 126, 134, 151–52, 167–76
- flux transfer events (FTEs), 84, 94, 103, 123, 137, 250
- Fokker-Planck model, 59, 63, 238
- Forbes, T., 16, 44
- Fourier analysis, 252–54
- fractals, 233–34
- frozen-in condition, 145
- galactic magnetic fields, 223–26
- Gaussians, 32
- geocentric solar magnetospheric (GSM) system, 219
- “Geospace Environmental Modeling (GEM) Magnetic Reconnection Challenge, The,” 69–73, 88
- geotail, 61, 86, 138, 185
- Giovanelli, R., 2, 30, 117

- global reconnection, 243, 247; co-helicity merging and, 103; current layer and, 165–66; impulsive, 127–28; self-organization and, 13, 28, 150–51, 157, 165–67; two-fluid effects and, 96
- global positioning system (GPS), 136
- guide field: astrophysical plasmas and, 134; concepts of magnetic reconnection and, 13; effects of, 51–52; energy flows and, 194–95, 202, 213; laboratory plasmas and, 100–101, 114, 170, 173; large systems and, 241, 242; magnetohydrodynamics (MHD) theories and, 47, 50–52; magnetopause and, 137, 139, 143; magnetotail and, 147; major findings and, 247; MRX and, 7, 52, 73, 84, 101, 170, 195, 218, 242; sawtooth crash and, 52; self-organization and, 170, 173; two-fluid theory and, 69, 73, 75, 84, 90, 93, 96–97, 217–19
- Hall effect: analytical description of reconnection layer and, 74–77; astrophysical plasmas and, 134; collisions and, 84; dynamos and, 163, 230–31; electron pressure and, 246; energy flows and, 178, 181, 184–85, 193–94, 203–5, 212–13; experimental measurements of, 81–83; fast reconnection and, 6, 13, 69, 71–72, 76–77, 84, 86, 96, 134, 181, 212–14, 243; future research and, 249; laboratory plasmas and, 113, 163; large systems and, 243; magnetohydrodynamics (MHD) theories and, 52; magnetopause and, 84–86, 137, 138–40; magnetotail and, 185; major findings and, 246; MRX and, 81–83; resistivity and, 69, 72, 78, 84, 89, 93–96; scaling data and, 94–96; self-organization and, 163; solar plasmas and, 134; two-fluid theory and, 66, 69, 71–78, 81–89, 93–96, 214–17
- Hamilton, R. J., 165
- Harris equilibrium, xii, 13; energy flows and, 205–10; experimental investigation of, 59–63; Fokker-Planck model and, 59, 63; generalized Harris sheet and, 56–59; kinetic theory and, 55–64; laboratory plasmas and, 55–56; Maxwell's equations and, 56–57, 59–64; MRX and, 59–64, 205; Ohm's law and, 61; plasma parameters and, 56; reconnection layer and, xi, 55–64; resistivity and, 61, 63–64; Sweet-Parker model and, 56, 63; X-point and, 61, 63; two-fluid theory and, 65, 71, 91
- heating: acceleration and, xi (*see also* acceleration); astrophysical plasmas and, 134; concepts of magnetic reconnection and, 1, 4, 6, 12; dynamos and, 227, 257; electron deposition and, 181–83; energy flows and, 177–78, 181–83, 187–88, 190, 196, 198, 208, 211; ions and, 187–90; laboratory plasmas and, 28, 104–9, 113–15, 151, 153, 164–66; large systems and, 241, 244; magnetohydrodynamics (MHD) theories and, 30; magnetopause and, *Color Plate* 8, 141–42, 145, 221; merging and, 104–9; NBI line and, 153; self-organization and, 151, 153, 164–66; solar flares and, 14–19; solar plasmas and, 118, 123; Takizuka-Abe particle-pairing algorithm and, 188; Thomson scattering and, 115; Tri-Alpha Energy (TAE) project and, 107–9; two-fluid theory and, 90, 187–90, 221, 222

- helicity: cohelicity, 50, 51, 102–3, 104, 111; conservation of, 165, 175, 230; counter, 102–4, 106, 111; laboratory plasmas and, 155–60, 162–65, 175; null, 50, 51, 111; opposite, 104; reversed field pinch (RFP) and, 26, 28, 159–62, 165, 230; self-organization and, 155–65, 175, 250; Sweet-Parker model and, 50; Taylor state and, 155–62, 175, 250
- heliospheric current sheets (HCSs), 130
- high- $\beta$  plasmas, 66, 88, 90–91, 103, 114, 115–16, 215, 240, 257
- Hinode satellite, 14, 18, 123–24
- hoop forces, 168, 175–76
- Horiuchi, R., 69
- Huang, Y, 235
- hybrid waves, 63, 90, 219, 257
- HYM code, 127
- IMP satellite, 62, 137
- International Astronomical Union (IAU), 31
- International Sun-Earth Explorer (ISEE), 62, 137
- interplanetary magnetic field (IMF), 5, 22–23, 51, 140
- ion diffusion region (IDR): energy flows and, *Color Plate 7*, 178, 181, 182, 189–90, 194, 199, 202–3, 211–13; large systems and, 238; magnetosphere and, 137–39, 142, 148; two-fluid theory and, 77–80, 84–88, 217–19, 222
- Ion Doppler spectroscopy, 106, 153
- ion dynamics spectroscopy probes (IDSPs), 106, 180, 187, 193–94, 196
- IRIS satellite, 14
- Ji, H., 50, 230, 241
- Kadomtsev model, 24–25, 26, 152–57
- kinetic reconnection: astrophysical plasmas and, 134; collisions and, 55–64; current sheet and, 56–58, 61–63; Fokker-Planck model and, 59, 63, 238; Harris equilibrium and, xii, 55–64; Klimontovich equations and, 56; Lundquist number and, 55; magnetosphere and, 21, 23, 55, 61–62, 140, 144, 146; Maxwell's equations and, 56–57, 59–64; MRX and, 59–64; multiple layers and, 238–40; neutral sheets and, 55–63; resistivity and, 61, 63–64; Sweet-Parker model and, 56, 63
- kinematic dynamos, 223, 227, 230
- Kliem, B., 20
- Klimontovich equations, 56
- Krall, N., 90
- KSTAR tokamak, *Color Plate 6*, 156
- Kulsrud, R., xiii, 36, 45, 61, 75–77, 83, 227, 251
- Kusano model, 248
- Landau damping, 90, 93, 257
- Langdon, A., 68
- Langmuir probes, 112, 113, 180, 185, 191, 193
- lasers, 88, 106, 114, 115–16, 223, 227, 240, 259
- Latham, J., 125, 127, 128
- layer aspect ratio, 202
- Lazarian-Vishnica model, 236–38
- Levinton, F. M., 153, 155
- Liewer, P., 90
- linear plasma device (LPD), 100, 102
- line-tied plasma: laboratory plasmas and, 114, 151, 167–76; self-organization and, 151, 167–76; solar plasmas and, 127; spheromak plasmass and, 127
- Lorentz force, 68–69, 121, 168, 184
- Loureiro, N., 234, 236, 241
- lower hybrid drift waves (LHDW), 91, 97
- lower hybrid waves (LHWs), 257
- Lu, E. T., 165

- Lundquist number, 259; concepts of magnetic reconnection and, 3; dynamos and, 228; energy flows and, 177, 199; equilibrium and, 248; fusion plasmas and, 23; kinetic theory and, 55; laboratory plasmas and, 28, 98, 101–2, 106, 152; large systems and, 232–38, 241–43; magnetohydrodynamics (MHD) theories and, 32, 40–42, 46, 50; major findings and, 248; self-organization and, 152; two-fluid theory and, 65, 215, 217
- Ma, Z. W., 69, 72, 96
- Mach probes, 82, 180, 187, 191, 193
- Madison Symmetric Torus (MST), 28, 162–65, 228
- magnetic annihilation, 17, 31, 106, 117
- magnetic diffusion, 2–3, 14, 30, 65, 89, 215
- magnetic energy transfer, 106, 148, 206, 207
- magnetic field lines: astrophysical plasmas and, 130, 132; connectivity and, 4–5, 14, 136, 238; dipoles and, 5, 21–23, 40, 46, 51, 64, 84, 86, 119, 136, 140, 191, 195, 214, 216–18, 223; energy flows and, 177–87, 191–95, 199, 203, 208, 211; flux freezing and, 78–79 (*see also* flux freezing); guide field and, 7 (*see also* guide fields); interplanetary magnetic field (IMF) and, 5, 22–23, 51, 140; measured flow vectors and, 180–81; MRX and, *Color Plate 1*; neutral points and, 4, 31, 38, 42; particle-in-cell simulations and, 68–69, 71–72, 130, 138, 181, 183, 188–89, 198, 205–12, 219, 220–21, 238; recent numerical simulation work on, 126–27; self-organization and, 152–57, 160, 164–68, 170, 176; solar plasmas and, 14–16, 117–29; two-fluid effects and, 71–72, 75–84, 88, 94, 214–19, 222; X-lines and, 12 (*see also* X-lines); X-point and, 10 (*see also* X-point); X-rays and, 2, 125, 129, 167
- Magnetic Reconnection eXperiment (MRX): xi, xiii; astrophysical plasmas and, 131; concepts of magnetic reconnection and, 7–10, 13; controlled driven reconnection experiments and, 109–12; dispersion and, 257; electron diffusion region (EDR) and, 148, 217–18, 250; electron flows in, *Color Plate 1*; energy flows and, *Color Plate 2*, 178–85, 188, 191–98, 202–7, 210–12; facility for, 109–12; field lines and, *Color Plate 1*; flow vectors and, 9, 192, 195, 216; flux ropes and, 20, 168–72, 238, 242–43; fusion plasmas and, 109; future research and, 250; guide field and, 7, 52, 73, 84, 101, 170, 195, 218, 242; Hall effect and, 81–83; Harris equilibrium and, 59–64, 205; Ion Dynamic Spectroscopy Probe and, 106; laboratory plasmas and, *Color Plate 3*, 7, 13, 20, 28, 29, 61, 79, 92–93, 96, 101, 106, 109–14, 131, 144–45, 168–71, 172, 178, 191, 198, 214–15, 241, 246; large systems and, 238, 241–43; magnetohydrodynamics (MHD) theories and, 46–52; magnetosphere and, 141, 144–45, 148, 196–97; Magnetosphere Multiscale Satellite (MMS) and, *Color Plate 1*, 9–10, 13, 79, 87, 97, 141, 144–45, 181, 194, 214–15, 217, 219–22, 246; major findings and, 246; particle-in-cell (PIC) simulations and, 205–12; scaling data and, 94–96; solar flares and, 20, 168–70; two-fluid theory and, *Color Plate 2*, 72–73, 79–97, 214–22



- magnetic relaxation, 20, 26, 28, 150, 158, 176
- magnetic topology, xi; cosmic rays and, 6; field-line, 1–3, 5, 15, 25, 36, 38, 41, 117, 122, 130, 165–67, 248; fusion plasmas and, 25; laboratory plasmas and, 101, 150–51, 165–69, 174; magnetohydrodynamics (MHD) theory and, 30–31, 36–38, 41; major findings and, 247–48; solar plasmas and, 14–15, 20, 117, 119, 122, 127–28, 130; two-fluid theory and, 73
- magnetohydrodynamics (MHD), xii, 13; acceleration and, 42, 52, 54; Alfvén waves and, 40–44; collisions and, 32–33, 46–47, 50–51; concepts of magnetic reconnection and, 1–13; coronal mass ejections (CMEs) and, 53; current sheet and, 31, 38, 42, 47–54; description of plasma in magnetic fields and, 32–33; diffusion and, 30, 37–40, 47–48; dynamos and, 224–26; early research on, 2–3; experimental analysis of the magnetic reconnection layer, 46–54; fast reconnection and, 31, 44, 46–47; field lines and, 30–41, 46–53; flux freezing and, 33–38; fusion plasmas and, 35–36, 41; guide field and, 47, 50–52; Hall effect and, 52; heating and, 30; historical perspective on, 30–31; ideal dynamics and, 3; ions and, 32, 42, 46, 52–54; kinetic theory and, 30–31, 38; laboratory experiments and, 30, 32, 34, 37–41, 44–51; Lundquist number and, 32, 40–42, 46, 50; magnetosphere and, 41–42, 46, 51; major questions of, 10–11; merging and, 38, 40, 47, 51, 53; MRX and, 46–52; neutral sheets and, 40–41, 47–48, 52; Petschek model and, 31, 42–46, 52–54; plasma density and, 33, 47; plasma parameters and, 33, 47; poloidal field (PF) and, 47, 49; reconnection layer and, 37, 39, 40, 42, 44, 46–54; resistivity and, 38–52; reversed field pinch (RFP) and, 35; solar flares and, 30–31, 38, 39, 41–42, 46; solar wind and, 41–42, 46, 52–54; space plasmas and, 46; spheromak plasmas and, 35; Sweet-Parker model and, 31–51; tension forces and, 41, 49, 54; tokamak plasmas and, 35, 52; toroidal field (TF) and, 47; two-fluid theory and, 66–68; X-lines and, 52, 53–54; X-point and, 31, 43–47, 48
- magnetopause: acceleration and, *Color Plate 8*, 145, 221; astrophysical plasmas and, 146–49; concepts of magnetic reconnection and, 5–13; diffusion and, 137, 138–43; electron-scale measurements of, 140–46; energy flows and, 190–91, 213; field lines and, 136–45; flux freezing and, 144–45; future research and, 250; guide field and, 137, 139, 143; Hall effect and, 84–86, 137, 138–40; heating and, *Color Plate 8*, 141–42, 145, 221; kinetic theory and, 55, 61–62, 140, 144; laboratory plasmas and, 109; magnetohydrodynamics (MHD) theories and, 42, 46; Magnetosphere Multiscale Satellite (MMS) and, *Color Plates 4–5*, 140–46; major findings and, 245; neutral sheets and, 136, 138; numerical simulations of, 137–40; particle-in-cell (PIC) simulations and, 138; plasma density and, 139, 142; plasma parameters and, 138; reconnection layer and, 135–46; solar winds and, 21–22; space plasmas and, 135–46; two-fluid theory and, 66, 84–86,

- 92, 94, 97, 214–22; X-lines and, 138–45, 146
- magnetosphere: astrophysical plasmas and, 135–49; collisions and, 23, 135, 138–40, 148; concepts of magnetic reconnection and, 1–13; current sheet and, 21–22, 136–37, 141, 146–48; diffusion and, 137, 138–43, 146–48; discovery of earth's, 135; dispersion and, 257; electron diffusion region (EDR) and, 23, 137, 139, 146, 148; electron-scale measurements of, 140–49; electron temperature and, 142; energy flows and, 177, 181, 191, 196–98; field lines and, 21–26, 28; future research and, 249; International Sun-Earth Explorer (ISEE) and, 62, 137; interplanetary magnetic field (IMF) and, 5, 22–23, 51, 140; ions and, 21, 23, 135, 137, 138–48, 196–97, 222; kinetic theory and, 21, 23, 55, 140, 144; laboratory experiments and, 31, 115, 141, 144–46; large systems and, 232, 243; magnetic reconnection in, 21–23, 135–49; magnetohydrodynamics (MHD) theories and, 41–42, 46, 51; Mars and, 135; MRX and, 141, 144–45, 196–97; neutral sheets and, 21; numerical simulations of, 137–40; potential wells and, 23; reconnection layer and, 23; solar plasmas and, 127–28, 133; solar wind and, 21–23, 135–37, 139; two-fluid theory and, 65–66, 69, 73, 79, 84–86, 214–15, 217–22; Venus and, 135; X-lines and, 22, 23
- Magnetosphere Multiscale Satellite (MMS), xii; electron diffusion region (EDR) and, 23, 148–49, 218–22; electron-scale measurements by, 140–49; energy flows and, 181, 190, 194–95; evolution of measured quantities by, *Color Plates 1–8*; findings of, 8; laboratory experiments and, 112; launching of, 8; magnetopause and, *Color Plates 4–5*, 140–46; magnetotail and, 146–49; major findings and, 246; MRX and, *Color Plate 1*, 9–10, 13, 79, 87, 97, 141, 144–45, 181, 194, 214–15, 217, 219–22, 246; TREX and, 113; two-fluid theory and, 79, 87, 96–97, 214–15, 217–18, 218–22; VTF experiment and, 112
- magnetotail: Alfvén waves and, 148; astrophysical plasmas and, 146–49; concepts of magnetic reconnection and, 8; diffusion and, 146–48; electron-scale dynamics of, 146–49; electron temperature and, 147, 148; energy flows and, 178, 184–87, 205–6; geotail and, 61, 86, 138, 185; guide field and, 147; Hall effect and, 185; kinetic theory and, 62, 146; laboratory plasmas and, 100, 112; magnetic reconnection in, 21; magnetohydrodynamics (MHD) theories and, 41; Magnetosphere Multiscale Satellite (MMS) and, 146–49; MRX and, 148; neutral sheets and, 148; plasma density and, 146; plasma parameters and, 146; potential wells and, 184–87; reconnection layer and, 146–49; solar flares and, 150, 152; solar wind and, 5; space plasmas and, 146–49; two-fluid theory and, 66, 86, 93; Wind spacecraft and, 138; X-lines and, 147–48
- Mars, 135
- Massachusetts Institute of Technology, 112
- Masuda, S., 17

- Maxwell's equations: dispersion and, 252, 254; electromagnetic dynamics of plasma fluids and, 32; energy flows and, 187, 189, 201; flux freezing and, 37; Harris equilibrium and, 56–57, 59–64; kinetic theory and, 56–57, 59–64; two-fluid theory and, 68; in vacuum, 5; Vlasov and, 56, 59, 64, 68, 201, 238
- mean field theory, 163, 223–25, 228–30
- merging: acceleration and, 104–6; antiparallel, 51, 102–3; astrophysical plasmas and, 130, 132; co-helicity, 51, 102–3; FRC plasmas and, 107–9; heating and, 104–9; Kusano model and, 248; laboratory plasmas and, 98, 102–9, 111, 114, 116; large systems and, 235; magnetohydrodynamics (MHD) theories and, 38, 40, 47, 51, 53; null-helicity, 51; Petschek model and, 103; solar plasmas and, 117–18, 123–27; SSX facility and, 106, 107, 114, 131; sunspots and, 117; Sweet-Parker model and, 38, 40, 103; TAE project and, 107–9; Today Spheromak-3 (TS-3) group and, 102–6; Tri-Alpha Energy (TAE) project and, 107–9
- microwaves, 17–18, 224
- MKSA units, 252, 258
- motional Stark effect (MSE), 153
- Mouikis, C. G., 69
- moving field lines, 80, 94, 179
- Mozer, F., 84–86, 138
- Myers, C. E., 168, 173, 175
- NASA, 129, 140
- neutral deuterium-beam injection (NBI), 153
- neutral points, 4, 31, 38, 42
- neutral sheets: astrophysical plasmas and, 133, 134; concepts of magnetic reconnection and, 5–6; energy flows and, 185–87, 199; kinetic theory and, 55–63; laboratory plasmas and, 28, 29, 98, 101, 106, 109, 111; large systems and, 240; magnetohydrodynamics (MHD) theories and, 40–41, 47–48, 52; magnetosphere and, 21, 136, 138, 148; solar plasmas and, 123; two-fluid theory and, 66, 70, 71–72, 73, 81–84
- neutrons, 17, 107, 132, 231
- Nilson, P. M., 115, 227
- null-helicity, 50, 51, 111
- numerical simulations, 56, 61, 65, 69, 86, 87, 123, 126, 137, 141, 183, 184–186, 205, 232
- Ohmic diffusion, 40, 78, 80, 96, 199, 237
- Ohmic dissipation, 31, 183
- Ohmic heating coils, 241
- Ohm's law: dynamos and, 226, 228, 230; energy flows and, 183, 193, 199; flux freezing and, 34, 37; Hall effect and, 246; Harris equilibrium and, 61; laboratory plasmas and, 163; large systems and, 237; Lundquist number and, 40; mean-field, 228, 230; toroidal current and, 50; two-fluid theory and, 67, 69, 71, 74–78, 80, 89, 96
- Omidi, N., 68
- onset of reconnection, 207
- Osborne, T., 154
- outflow velocity, 87, 88, 128, 202, 212
- pair plasma, 132, 242–43, 249
- paramagnetic (effects), 170, 173–74, 176
- Parker, E., 31
- Parker Solar Probe (PSP), 14, 129–30
- particle detectors, 101
- particle-in-cell (PIC) simulations: astrophysical plasmas and, 130; energy flows and, 181, 183, 188–89, 198, 205–12; Harris equilibrium and, 205; large systems and,

- 238; magnetopause and, 138; MRX and, 205–12; two-fluid theory and, 68–69, 71–72, 219, 220–21
- Petschek model, 11; acceleration and, 52–54; Biskamp simulation and, 44; collisions and, 84; energy flows and, 178; future research and, 245; laboratory plasmas and, 101, 103; large systems and, 232–33; Lundquist number and, 46; magnetohydrodynamics (MHD) theories and, 31, 42–46, 52–54; merging and, 103; shocks and, 43, 45; Sweet-Parker model and, 31, 42–46; two-fluid theory and, 72, 83–84
- Phan, T., 130
- photosphere, 14–20, 84, 121–23, 166
- Plasma Science and Fusion Center, 112
- plasma sheet, 5, 61, 63, 99, 136, 137, 139, 146
- plasma transport, 72, 249
- plasma turbulence, 126
- plasmoid theory, 232–36
- poloidal field (PF): dynamos and, 230; energy flows and, 179, 203; fusion plasmas and, 24; laboratory plasmas and, 27, 157, 160; magnetohydrodynamics (MHD) theories and, 47, 49; self-organization and, 157, 160; two-fluid theory and, 79, 109, 217
- potential wells: energy flows and, 181, 184–87, 188, 196, 208–11; ion energy increase and, 208–11; magnetosphere and, 23; magnetotail and, 184–87; two-fluid theory and, 79, 86, 221
- Poynting flux, 199–200, 203, 205–7, 212–13
- Priest, E., 16, 44
- Princeton Plasma Physics Laboratory (PPPL), xi, 109, 113–14, 241, 251
- Pritchett, P., 68–71
- protons: kinetic theory and, 62; laboratory plasmas and, 115; solar plasmas and, 17; space plasmas and, 259; two-fluid theory and, 95
- q*-profile, 25, 153, 155–56
- quantum computing, 250
- quasi-neutrality condition, 58, 76
- rapid reconnection. *See* fast reconnection
- Rappasso, A. F., 165
- reconnection layer: astrophysical plasmas and, 130, 132–34; concepts of magnetic reconnection and, xi, 3, 6–13; dispersion and, 257; energy flows and, 177–81, 184–91, 194–202, 207–13; fusion plasmas and, 24; future research and, 249–50; Harris equilibrium and, xi, 55–64; kinetic theory and, 55–64; laboratory plasmas and, 28–29, 102, 109–10, 115, 116, 150, 157, 166–68; large systems and, 232, 236–40, 243; magnetohydrodynamics (MHD) theories and, 37, 39, 40, 42, 44, 46–54; magnetopause and, 135–46; magnetosphere and, 23, 135–49; magnetotail and, 146–49; major findings and, 245–48; self-organization and, 150, 157, 166–68; solar plasmas and, 15–16, 20, 123; two-fluid theory and, 65, 69, 73–96, 214–17, 222
- Reconnection Scaling Experiment, 113
- relativistic reconnection, 12, 130, 132, 200, 224, 238
- Ren, Y., 94
- resistivity: concepts of magnetic reconnection and, 3; dynamos and, 225–26; energy flows and, 183, 198–201; enhanced, 44, 47, 63, 89–97, 232–33, 236, 240, 250, 257; Hall effect and, 69, 72, 78, 84, 89, 93–96; Harris equilibrium

- resistivity (*continued*)  
and, 61, 63–64; kinetic theory and, 61, 63–64; laboratory plasmas and, 101; large systems and, 232–37, 240; lower hybrid frequency range and, 250; magnetohydrodynamics (MHD) theories and, 30, 32, 34, 37–52; solar plasmas and, 122–23, 129; two-fluid theory and, 69, 72, 78, 84, 89–97
- Reuven Ramaty High-Energy Solar Spectroscopic Imager (RHESSI), 14, 17
- reversed field pinch (RFP), 13, 103; concepts of magnetic reconnection and, 12; configuration formation of, 160–61; dynamos and, 223, 227–31; early laboratory experiments on, 98–99; energy flows and, 178; fast reconnection and, 12; fusion plasmas and, 23–26, 28; future research and, 249–50; helicity and, 26, 28, 159–62, 165, 230; laboratory plasmas and, 27, 152, 157–65, 167, 176; large systems and, 244; magnetic relaxation and, 26, 28; magnetohydrodynamics (MHD) theories and, 35; major findings and, 248; sawtooth oscillations and, 162–65; self-organization and, 152, 157–65, 167, 176; solar plasmas and, 120–21, 129; spheromak plasmas and, 157–67; tokamak plasmas and, 153–65; TPE-IRM20 and, 230; two-fluid theory and, 96
- Richardson diffusion, 237
- RLC capacitor, 170
- Rotating Wall Experiment, 113
- Sato, T., 69
- sawtooth oscillations: crash phase of, 25, 26, 52, 94, 129, 153–57, 162, 167, 248; fusion plasmas and, 23–26; Kadomtsev model and, 24–25, 26, 152, 154–55, 157; large systems and, 244; physical processes during, 155–57;  $q$  profiles and, 25, 153, 155–56; reconnection on tokamaks and, 152–57; reversed field pinch (RFP) and, 162–65; solar plasmas and, 129; Sweet-Parker model and, 157; thermal energy and, 129, 155, 167, 248; two-fluid theory and, 94
- scattering, 96, 101, 115, 146
- Science News*, 130
- SDO satellite, 14
- self-organization, x, 151; Center for Magnetic Self-Organization (CMSO), 251; magnetic self-organization, 129
- separatrix, separatrices: energy flows and, 179, 181–97, 199, 208, 211, 213; magnetopause and, 137, 142; solar plasmas and, 123, 125; two-fluid effects and, 71–72, 76, 77, 80, 81–82, 84, 93, 96, 217
- Shay, M., 69, 219
- Shibata, K., 17–19, 125, 233–34
- Skylab, 14
- SOHO satellite, 14
- solar flares: acceleration and, 16–18; Alfvén waves and, 17, 19–20, 127–30; astrophysical plasmas and, 20, 131, 133–34; breakout model and, 123–27; chromosphere jets and, 123–24; concepts of magnetic reconnection and, 1–3, 13; coronal mass ejections (CMEs) and, xi, 1, 13–17, 20, 117, 119, 120, 123–25, 126, 129, 247–48; CSHKP model and, 15–17, 121–23; energy buildup and, 117–19; energy flows and, 177; equilibrium and, 15–16, 20, 119–22, 126–29; flux concentrations and, 14–15; flux ropes and, 16, 20, 120–22, 126, 134, 151–52, 167–76; heating and, 14–19; laboratory eruption studies and, 167–76;

- laboratory plasmas and, 106, 113, 115; large systems and, 232–34, 236, 243–44; limitation of MHD models and, 129; low altitude, 18–20; magnetic reconnection in, 1–3, 13–21, 117–19; magnetohydrodynamics (MHD) theories and, 30–31, 38, 39, 41–42, 46; magnetotail and, 150, 152; major findings and, 247–48; MRX and, 168–72; multipolar magnetic configuration and, 123–27; new interpretation of, 124–25; new model for, 125–27; photosphere and, 14–20, 84, 121–23, 166; plasmoid theory and, 232–36; pre-eruption configurations and, 119–21; prominence eruptions and, 15; recent numerical simulation work on, 126–27; satellites and, 14; self-organization and, 1, 13, 129, 150, 152, 165–75, 243–44, 247–48; standard model for, 119–23; thermal energy and, 14–15, 17, 129; two-fluid theory and, 84; X-lines and, 16; X-point and, 16, 128
- Solar Optical Telescope (SOT), 18
- solar plasmas, xii; line-tied plasma and, 127; spheromak plasmas and, 121, 125–27; Sweet-Parker model and, 14, 17, 118, 123, 129; tokamak plasmas and, 129
- solar reconnection, 53, 73
- solar wind: Alfvén waves and, 19, 130; concepts of magnetic reconnection and, 1, 5–8; energy flows and, 177, 191, 213; magnetohydrodynamics (MHD) theories and, 41–42, 46, 52–54; magnetosphere and, 5, 21–23, 135–37, 139; major findings and, 245; radial direction of, 132; Sturrock model and, 119; two-fluid theory and, 65, 86, 214–15
- Sonnerup, B., 75
- space plasmas: concepts of magnetic reconnection and, xi, 5, 11, 13; energy flows and, 199, 205–6; kinetic theory and, 62; magnetohydrodynamics (MHD) theories and, 46; magnetopause and, 135–46; magnetotail and, 146–49; major findings and, 246–47; protons and, 259; self-organization and, 159
- spheromak plasmas: astrophysical plasmas and, 131; configuration formation of, 161–62; dynamos and, 223, 229; energy flows and, 178; fusion plasmas and, 23–24; laboratory plasmas and, 98, 102, 105–9, 152, 157–65, 167, 170, 176; line-tied plasma and, 127; magnetohydrodynamics (MHD) theories and, 35; recent numerical simulation work on, 126–27; reversed field pinch (RFP) in, 157–65, 167; self-organization and, 152, 157–65, 167, 176; solar plasmas and, 121, 125–27; SSX facility and, 106, 107, 114, 131; Todai Spheromak-3 (TS-3) group and, 102–6; toroidal, 102–6
- Spitzer resistivity, 47, 50–51, 78, 95–96, 183
- Stoke's theorem, 35
- storage-and-release model, 15, 20, 117, 151, 168–70
- Sturrock, P. A., 118–19, 121
- substorms, 21–23, 65, 131, 136, 185, 243
- sunspots, 2, 18, 30, 38, 40, 117, 123
- superparticles, 69
- Swarthmore Spheromak Experiment (SSX) facility, 106, 107, 114, 131
- Sweet, J., 31
- Sweet-Parker model: Alfvén waves and, 40–42; Biskamp simulation and, 44; collisions and, 84, 241–42; current sheet and, 11, 31, 41–46, 55–56, 63, 83, 165, 232–35, 238, 240, 242; energy deposition and,

- Sweet-Parker model (*continued*)  
212–12; energy flows and, 177, 198–203, 211–12; enhanced resistivity and, 89, 95–96; experimental test of, 46–47; future research and, 249; Harris equilibrium and, 56, 63; helicity and, 50; Ji generalization of, 50; kinetic theory and, 56, 63; laboratory plasmas and, 29, 46–47, 155–57, 165, 167; large systems and, 232–42; Lundquist number and, 40–42, 46, 235–36; magnetohydrodynamics (MHD) theories and, 31–51; major findings and, 245–48; merging and, 38, 40, 103; multiple reconnection layers and, 238; Petschek model and, 31, 42–46; physical interpretation of, 41–42; plasmoid theory and, 233; progress from, 245; sawtooth oscillations and, 157; scaling data and, 95–96; self-organization and, 155–57, 165, 167; solar plasmas and, 14, 17, 118, 123, 129; turbulence and, 237; two-fluid theory and, *Color Plate 3*, 66, 71–75, 78, 83–84, 89, 95–96
- synchrotron radiation, 17, 132, 225,
- Tajima, T., 234
- Takizuka-Abe particle-pairing algorithm, 188
- Tanuma, S., 232–34
- Taylor state, 158–62, 175, 250
- tension forces: concepts of magnetic reconnection and, 3–4; energy flows and, 177; laboratory plasmas and, 170, 175–76; magnetohydrodynamics (MHD) theories and, 41, 49, 54; self-organization and, 170, 175–76
- Terasawa, T., 75
- Terrestrial Reconnection EXperiment (Trex) facility, 113, 114
- TEXTOR tokamak, *Color Plate 6*, 156
- Thomson scattering, 115
- three-dimensional reconnection, 11, 13, 246; energy flows and, 181, 194; impulsive, 243; kinetic simulations and, 238; laboratory plasmas and, 106, 109, 113, 164; magnetosphere and, 24, 140, 145, 149; MHD theories and, 42, 52; numerical theories and, 232; solar plasmas and, 16, 122–23, 125, 129; two-fluid effects and, 88, 93, 222
- Today Spheromak-3 (TS-3) group, 102–6
- Tokamak Fusion Test Reactor (TFTR), 25, 154–55
- tokamaks: concepts of magnetic reconnection and, 3; dynamos and, 227; electron temperature and, 153–54; equilibrium and, 152–53, 157, 167, 170, 248; fusion plasmas and, 23–26; future research and, 249–50; Kadomtsev model and, 24–25, 26, 152, 154–55, 157; KSTAR, *Color Plate 6*, 156; laboratory plasmas and, 98, 152–58, 167, 170; large systems and, 243; magnetohydrodynamics (MHD) theories and, 35, 52; major findings and, 248; reversed field pinch (RFP) and, 157–65; sawtooth reconnection in, 152–57; self-organization and, 152–58, 167, 170; solar plasmas and, 129; TEXTOR, *Color Plate 6*, 156; two-fluid theory and, 94, 96
- toroidal field (TF): energy flows and, 179; fusion plasmas and, 24, 26; laboratory plasmas and, 27, 102–6, 109–11, 152–53, 156–60, 168, 170, 173–76; Lorentz force and, 68–69, 121, 168, 184; Madison Symmetric Torus (MST) and, 228; magnetohydrodynamics (MHD) theories and, 47; plasma merging and, 102–9; reversed field pinch (RFP) and, 153–65; spheromak plasmas and,

- 153–65; tokamaks and, 153–65; Tri-Alpha Energy (TAE) project and, 107–9; two-fluid theory and, 79, 84, 217; Versatile Toroidal Facility (VTF) and, 93, 112–13, 114
- Török, T., 20
- TRACE satellite, *Color Plate 1*, x, 2, 14, 17
- Tri-Alpha Energy (TAE) project, 107–9
- Tsuda, T., 45
- turbulent reconnection, 83, 94, 113, 236–38, 249–50
- two-dimensional reconnection, 5–8, 243, 246; energy flows and, 184, 194, 208; kinetic, 59, 61, 63; laboratory plasmas and, 28, 103, 109, 111, 122–23, 156–57; magnetosphere and, 138, 141–42, 145, 148–49; MHD theories and, 38, 40–42, 45, 50; numerical theories and, 232; solar flares and, 16; Sweet-Parker model and, 235, 238; two-fluid effects and, 65, 69–77, 80–86, 96–97, 216–17
- two-fluid effects: Alfvén waves and, 65, 87, 90, 215, 219; collisions and, 65–84, 87–97, 214–18; Coulomb interactions and, 68, 78–79, 217; current sheet and, *Color Plate 3*, 79–84, 90–94, 97, 214, 216; electric potential well and, 184–87; electron diffusion region (EDR) and, 72, 76–80, 85, 86–89, 94, 96–97, 214–22; electron outflow and, *Color Plate 3*, 87; electron pressure and, 73, 75, 78, 83, 96; energy flows and, *Color Plate 7*, 185, 201–5; fast reconnection and, 13, 69, 72, 84, 91, 96, 214; field lines and, 71–72, 75–84, 88, 94, 214–19, 222; flux freezing and, 75, 78–79, 219; guide field and, 69, 73, 75, 84, 90, 93, 96–97, 217–19; Hall effect and, 66, 69, 71–78, 81–89, 93–96, 214–17; Lorentz force and, 68–69; Lundquist number and, 65, 215, 217; magnetopause and, 65–66, 69, 73, 79, 84–86, 92, 93–94, 97, 214–22; Magnetosphere Multiscale Satellite (MMS) and, 79, 87, 96–97, 214–22; MRX and, *Color Plate 2*, 72–73, 79–97, 214–22; neutral sheets and, 66, 70, 71–72, 73, 81–84; particle-in-cell (PIC) simulations and, 68–72, 219, 220–21; Petschek model and, 72, 83–84; poloidal field (PF) and, 79, 109, 217; potential wells and, 79, 86, 221; resistivity and, 69, 72, 78, 84, 89–97; reversed field pinch (RFP) and, 96, 178; solar wind and, 65, 86, 214–15; Sweet-Parker model and, 66, 71–75, 78, 83–84, 89, 95–96; Takizuka-Abe particle-pairing algorithm and, 188; thermal energy and, 93, 218–19, 222; toroidal field (TF) and, 79, 84, X-lines and, 75, 93, 96, 214, 216, 217–19, 221; X-point and, 71–72, 77–83, 86, 217; X-rays and, 84, 117, 122–29
- Ugai, M., 45
- Uzdensky, D., 45, 75–77, 83, 132, 236, 241, 251
- Vasyliunas, V., 44
- vector potential, 57, 100, 101, 159
- Vela satellite, 137
- Venus, 135
- Versatile Toroidal Facility (VTF), 14, 93, 112–13, 114
- Vishniac, E., 236–38
- Vlasov equations, 56, 58, 59, 64, 68, 80, 201, 238
- von Goeler, S., 24
- VPIC code, 183, 188, 205, 238



- Wang, Y., 90  
whistler waves, 72, 90, 97, 101, 219, 257  
Wind satellite, 52, 53–54, 86, 112, 138  
Winske, D., 68  
Wyper, P., 125, 126
- X-lines, 12; astrophysical plasmas and, 134; energy flows and, 106, 185–87, 188, 191, 194–95, 211; future research and, 249; laboratory plasmas and, 113; large systems and, 240–41; magnetohydrodynamics (MHD) theories and, 52, 52–54; magnetosphere and, 22, 23, 138–48; major findings and, 246; solar flares and, 16; two-fluid theory and, 75, 93, 96, 214, 216, 217–19, 221  
X-point: astrophysical plasmas and, 134; concepts of magnetic reconnection and, 10; energy flows and, 178, 180–84, 189, 192, 194; Harris equilibrium and, 61, 63; kinetic theory and, 61, 63; laboratory plasmas and, 28, 100, 110; large systems and, 232, 242; magnetohydrodynamics (MHD) theories and, 31, 43–47, 48; major findings and, 246; solar flares and, 16, 128; two-fluid theory and, 71–72, 77–83, 86, 217  
X-rays: astrophysical plasmas and, 131; concepts of magnetic reconnection and, 2; field lines and, 2, 125, 129, 167; fusion plasmas and, 24–25; laboratory plasmas and, 106, 167; self-organization and, 167; solar plasmas and, 14, 16–19, 247; TRACE satellite and, *Color Plate 1*, 2; two-fluid theory and, 84, 117, 122–29
- Yamada, M., 8, 10, 12, 26, 29, 35, 46–48, 79–84, 102, 125–27, 194, 202, 208, 242  
Yohkoh satellite, 14–18, 121, 125  
Yokoyama, T., 18  
Yoo, J., 191–93, 198, 205, 208, 213, 257  
Zweibel, E., 12, 224, 226